POS 522 Cruise Report

R.V. Poseidon cruise no. 522

Dates, Ports: 10.04.2018 (Catania, Italy) – 29.04.2018 (Malaga, Spain)

Research subject: Tephrostratigraphy of tsunami-related deposits at Stromboli

Chief Scientist: Dr. Armin Freundt, GEOMAR, Kiel

Number of Scientists: 11

Project: Stromboli tsunamis

Alphabetical list of participating scientists:

Name	Affiliation
Giacomo Dalla Valle	ISMAR, Bologna
Alessio di Roberto	Universita di Pisa
Kai Fockenberg	GEOMAR, Kiel
Armin Freundt	GEOMAR, Kiel
Kevin Krohne	GEOMAR, Kiel
Michael Marani	ISMAR, Bologna
Alessandra Mercorella	ISMAR, Bologna
Asmus Petersen	GEOMAR, Kiel
Marco Pistolesi	Universita di Pisa
Mauro Rosi	Universita di Pisa
Marija Voloschina	GEOMAR, Kiel

POS 522 scientific party – back row, from left to right: Alessio di Roberto, Alessandra Mercorella, Michael Marani, Asmus Petersen, Giacomo dalla Valle, Kevin Krohne, Mauro Rosi; front row: Marija Voloschina, Armin Freundt, Marco Pistolesi, Kai Fockenberg.

1. Acknowledgements

2. Introduction

Stromboli volcano in the Aeolian archipelago is world famous for its continuous volcanic activity throughout historic times. It is less well known as a source of tsunamis that threaten coasts around the Tyrrhenian Sea, and are generated by flank collapses. The last tsunami occurred in 2002, five such events occurred during the last century, and at least four major collapses occurred over the past 13 ka. Useful landslide and tsunami hazard assessment requires a record of past ages, frequencies, mechanisms and magnitudes of collapse events. The aim of this cruise was to determine that record by sampling sediment profiles on the seafloor north of Stromboli where the distal turbidites of proximal landslide masses have been deposited. Next to the stratigraphic succession, we wanted to observe lateral facies variations by an array of drill cores because these are particularly indicative of the dynamic processes. Three seamount complexes exist near Stromboli with bathymetric indication for collapse structures but otherwise practically unknown. Shipboard bathymetric mapping and water (CTD) and rock (dedge) sampling have been employed to characterize collapse structures and magmatic compositions, and search for hydrothermal signs of volcanic activity.
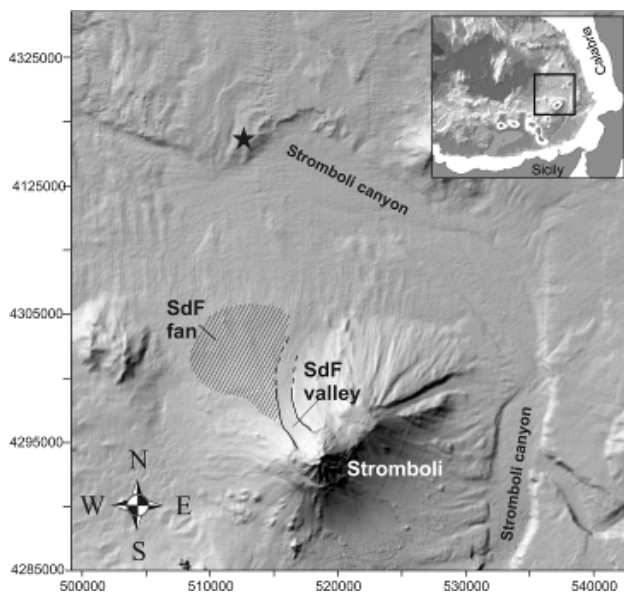

Fig. 1: Shaded relief bathymetry of the Stromboli region highlighting the main features of the Stromboli submarine sedimentary system; the star marks the sampling site of Di Roberto et al. (2010). Inset shows location of Stromboli Island within the south Tyrrhenian sea. SdF is the Sciara del Fuoco and its submarine fan. Below: Relief of Stromboli from Tinti et al. (2005).

3. Background

Stromboli, in the Aeolian archipelago, is located in the Southern Tyrrhenian Sea, a few tens of kilometers offshore from the north coast of Sicily and the Italian peninsula (Fig. 1). The island, with an elevation of 924 m asl, represents the subaerial part of a larger volcanic edifice extending to a maximum water depth of 2,600 m bsl. Stromboli volcano was built during seven main periods of activity covering a time span of about 100 ka, separated by caldera and flank collapses (Fig. 2).

The most striking geomorphological and volcanic structure of the island is the Sciara del Fuoco (SdF; Fig. 1), a horseshoe-shaped collapse scar that occupies the NW sector of the island. The SdF structure is considered the result of at least four flank collapses that occurred in the last 13 ka (Figs. 2, 3; Tibaldi, 2001). The SdF structure continues below sea level (Fig. 1) as a depression bounded by steep walls in continuity with the flanks of the sub-aerial SdF (Kokelaar and Romagnoli, 1995). This structure acts as a collector for the materials involved in the flank instability events, funneling them toward the Stromboli canyon,
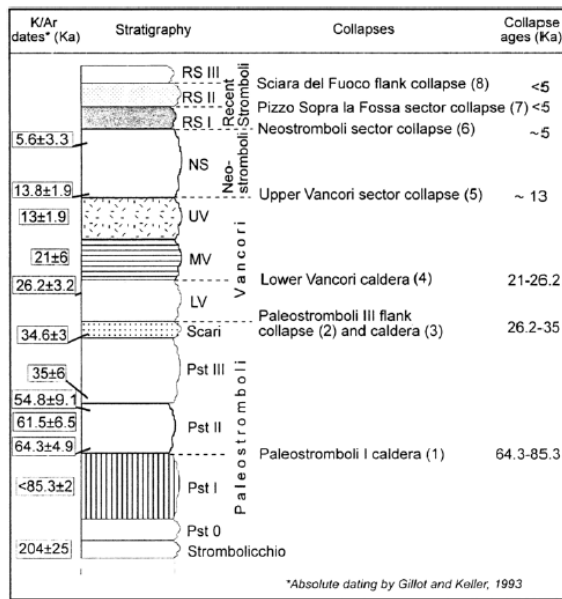
a huge erosional channel that originates on the northern Sicilian continental slope. The SdF was the source of the last landslide event of December 2002.

Fig. 2: Ages and stratigraphic profile of Stromboli volcano with the major collapse events from Tibaldi (2001).

Tsunami hazard at Aeolian Islands

More than 60% of Italian population and the majority of productive facilities are concentrated along the coasts of the peninsula and are thus exposed to tsunami risk. Tsunami waves resulting from volcanic eruptions and mass failures (subaerial and submarine landslides) have historically affected the coasts of Italy and in particular of the southern Tyrrhenian Sea. Most of tsunamis of the Tyrrhenian Sea (seven in the last century) originated from the volcanic islands of Stromboli and Vulcano, and were mainly associated with volcanic landslides (Tinti et al., 1999, 2000; Maramai et al., 2005a, b). The event on 30 December 2002 showed that collapses much smaller than the major events depicted in Fig. 2 can be tsunamigenic. In 2002, landslides with a total volume of about $25–30x10^6$ m^3 (Marani et al., 2008a) detached from the NW flank of Stromboli volcano, and resulting tsunami waves up to 10 m high struck the coasts of Stromboli causing severe damage to the Stromboli village. Waves up to 2 m high reached the neighboring islands (Tinti et al., 2005) and further propagated toward the northern coasts of Sicily, weakly affecting the Milazzo harbor 100 km south of Stromboli (Maramai et al., 2005a, b). As a result of the 2002 event the Italian Department of Civil Protection set up a contingency plan in 2015 for a tsunami event at Stromboli that is calibrated on the 2002 scenario which is considered as the most hazardous one (high-frequency, mid-scale event). However, little is yet known about the frequency and magnitudes of past tsunami events. This past record needs to be recovered and investigated in order to be able to also implement emergency plans for larger, less-frequent events.

Assessing the tsunami record through landslide depositional facies

Paleo-tsunami deposits can be found in coastal sediment successions but are commonly incompletely exposed due to the highly erosive environment. Moreover it is difficult to distinguish tsunami deposits from storm deposits (tempestite). Preservation potential is much better in the submarine environment where the deposits of large-scale landslides are commonly associated with deposits of turbidity currents. It is well known that collapse events do not only leave coarse-grained debris avalanche deposits on the seafloor but that the partial mixing of the slide mass with the surrounding seawater can form turbulent density (turbidity) currents charged with fine volcaniclastic sediment (Hampton, 1972; Garcia et al., 1994; Garcia, 1996). These currents can travel and laterally spread for hundreds of kilometers leaving deposits on vast areas of the deep ocean floor (Carey et al., 1998; Piper et al., 1999; Hunt et al., 2014, 2015). Because mass and dispersal characteristics of turbidity current deposits can be considered as a proxy of volume and energy of the landslides (e.g., Hunt et al., 2014, 2015) they can also be considered a proxy of the resulting tsunami waves (e.g., Murty, 2004). Northwest of Stromboli, Marani et al. (2008a, b) and Di Roberto et al.

(2010) have actually documented three submarine deposit facies associated with mass wasting by sidescan sonar and video mapping and sampling: (1) The chaotic, very coarse-grained proximal landslide deposit with breccia mounds is followed, and partly overlain, by (2) a sand to granule size volcaniclastic sediment composed of cross-bedded and massive layers and capped by ripple structures (Fig. 5) that is thought to have been emplaced by cohesionless granular flow. (3) Volcaniclastic turbidites form the distal facies. Marani et al. (2008a, b) observed facies (2) locally on the downstream side of facies (1) mounds but generally the distribution of, and the transitions between, the three facies are poorly known. This also holds for lateral variations in composition because of the limited previous sampling stations. The sediment cores collected during cruise POS 522 will be particularly used to investigate lateral variations in the turbidite deposits.

Marine tephrochronostratigraphyand compositional correlations
We also found primary fallout ash layers in the sediment cores that may be derived from stronger explosive eruptions at Stromboli, other Aeolian islands, Etna, Vesuvius or Campi Flegrei. Geochemical correlation (mainly based on glass geochemical compositions) of these ash layers as well as of cryptotephras dispersed in the marine sediments with known and dated tephras on land can provide important time lines for the marine sediment stratigraphy. Di Roberto et al. (2010) analyzed a 1-m-long core collected north of Stromboli and showed that the turbidite deposits can be correlated with compositionally distinct phases in the magmatic evolution of Stromboli over the past ca. 15 ka.

4. Cruise Narrative

4.1 Daily Narrative

(see station list 4.2 and station map 4.3 below)
April 10: At 9:15 the ship left Catania harbor and reached the first work station at Lemetini NE seamount at 20 h to begin the nighttime bathymetric mapping (station 1).
April 11: Stations 2 to 6
After a CTD deployment (St. 2) in the morning at Lemetini, we collected the first two cores on the plateau north of Stromboli (St. 3, 4). We quickly faced the difficulties of penetrating near-surface sand layers because after 4 m recovery at St. 3 we got zero penetration and recovery at St. 4. We concluded the day with another CTD (St. 5) and continued mapping (St. 6) at Lemetini NE.
April 12: Stations 7 to 12
Coring stations 7 to 11 yielded nothing but a bend pipe because we could not achieve any penetration into the sediments close to the southern rim of the plateau. In the evening we continued mapping (St. 12) at Lemetini NE.
April 13: Stations 13 to 16
We tried variations in tube length and impact speed but still had no success with coring at Stations 13 and 14 at the southern rim. Since this time we did not have the scissor system for free-fall entry available which served us very well on cruise POS 513, the possibilities to try for better penetration were limited. We concluded the day with another CTD and mapping at Lametini SW (St. 15, 16).
April 14: Stations 17 to 21
We moved further westward along the south rim of the plateau but found the same conditions at coring stations 17-19 which delivered no recovery. Hence we turned to No-Name E seamount for CTD and mapping (St. 20, 21).
April 15: Stations 22 to 24

Moving a bit north off the southern edge of the plateau, we finally got 2.5 m recovery at St. 22 but again none at St. 23. We then took a long leg to map at Alcione seamount (St. 24).

April 16: Stations 27 to 31

Finally stations 27-29 on the east side of the plateau and about 10 km from the southern rim gave good core recoveries from 2.5 to 4.5 m. Stations 30 (CTD) and 31 (mapping) took us back to Alcione seamount for the night.

April 17: Stations 32 to 37

An E to W traverse of four core stations (32-35) across the central plateau yielded core lengths from 1.6 to 3.1 m, sufficient to capture the Holocene turbidite sequence and to relieve the frustration from the first days. Evening CTD and nighttime mapping again at Alcione (St. 36, 37).

April 18: Stations 38 to 42

Another coring traverse across the plateau (St. 38-40) was even more successful than the previous day when yielding 5.8 to 6.7 m recoveries. With such long cores we have good chances to record a number of late Pleistocene events. Evening CTD and nighttime mapping again at Alcione (St. 41, 42).

April 19: Stations 43 to 45

During the night we had moved to the eastern rim of the Marsili basin in order to collect two cores in those deep waters (St. 43, 44), each of which gave 2.4 m recovery. For nighttime mapping we returned to Lametini NE seamount (St. 45).

April 20: Stations 46 to 49

A northerly E-W traverse of three cores (St. 46-48) across the plateau yielded excellent recoveries of 5.5 to 7.5 m. Nighttime mapping at Lametini SW seamount (St. 49).

April 21: Stations 50 to 54

A CTD near Lametini SW (St. 50) was followed by three gravity coring stations. Station 51 immediately south of Lametini NE seamount delivered a 1.8 m core but the other two stations (52, 53) on the western part of the plateau yielded no recovery. Mapping at Lametini SW seamount continued over night (St. 54).

April 22: Stations 55 and 56

On this day we cored at two stations far apart. Station 55 at the western slope of the plateau into the Marsili basin achieved no penetration but station 56 in the northeastern Marsili basin recovered 1.8 m core. Overnight took the long transfer to the No-Name seamounts, target of the final work day.

April 23: Stations 57 and 58

The final work days were reserved for dredging at the No-Name seamounts. The seamounts are obviously thickly covered in mud so that only dredge station 58 did actually sample hard rock fragments.

April 24: Stations 59

The third dredge taken early in the morning again only recovered mud so that by about 9 h we concluded the scientific program and made our way towards Malaga harbor which we entered early morning on **April 28**. Unloading the same day went smoothly and the scientific crew finally disembarked on the morning of **April 29**.

Overall, we worked 57 stations during cruise POS 522, including 34 gravity corer deployments of which 21 delivered cores, 8 CTD stations, 12 multibeam bathymetric mappings of three seamount complexes, and 3 barrel dredge tracks. The sediment cores range from 1.5 to 7.5 m lengths yielding a total 73 m core length and are packed full with turbidite and ash layers so that several hundred volcaniclastic layers will have to be analyzed during the continuation of this project.

Stationlist POS 522

GC= gravity corer
3 = 3 m tube
5 = 5 m tube
8 = 8 m tube

Bathy = bathymetric mappings

Note: station numbers 25 and 26 have not been used

| Station	Instrument	Date	Time UTC	Latitude (N)	Longitude (E)	Water depth	max. rope tension (kN)	Penetration	Recovery
	Time UTC = ship time		Begin of station				Coring parameter		
1	Bathy	10.04.18	20:00						
2	CTD	11.04.18	06:08	39° 00.673	15° 26.445	2120			
3	GC5	11.04.18	09:50	39° 05.014	15° 13.550	2350	80	4	3,97
4	GC5	11.04.18	12:02	39° 04.909	15° 08.566	2498	64	0	0
5	CTD	11.04.18	14:40	39° 04.182	15° 19.644	2264			
6	Bathy	11.04.18	16:00						
7	GC5	12.04.18	06:00	39° 03.985	15° 16.635	2320	62	2	1,63
8	GC5	12.04.18	08:05	39° 04.501	15° 16.132	2299	63	0	0
9	GC5	12.04.18	11:00	39° 04.842	15° 11.151	2470	62	0	0
10	GC5	12.04.18	13:10	39° 02.650	15° 10.952	2456	60	0	0
11	GC3	12.04.18	14:50	39° 02.649	15° 10.915	2456	60	0	0
12	Bathy	12.04.18							
13	GC3	13.04.18	11:38	39° 02.113	15° 15.560	2390	60	0,2	0,2
14	GC3	13.04.18	13:25	39° 02.902	15° 12.962	2408	60	0	0
15	CTD	13.04.18	15:23	39° 02.004	15° 16.196	2377			
16	Bathy	13.04.18							
17	GC3	14.04.18	06:00	39° 01.797	15° 07.440	2538	62	0	0
18	GC3	14.04.18	08:15	39° 02.953	15° 07.776	2513	62	0	0
19	GC3	14.04.18	11:00	39° 01.436	15° 05.637	2567	73	0	0
20	CTD	14.04.18	13:50	38° 57.426	15° 06.504	2662			
21	Bathy	14.04.18							
22	GC3	15.04.18	11:00	39° 03.365	15° 05.661	2593	70,5	2,5	2,23
23	GC3	15.04.18	13:34	39° 07.294	15° 07.124	2534	63	0	0
24	Bathy	15.04.18							
27	GC3	16.04.18	07:00	39° 06.738	15° 20.179	2026	67	1,5	1,45
28	GC3	16.04.18	08:30	39° 05.520	15° 18.711	2214	78	3,3	3
29	GC5	16.04.18	11:03	39° 05.517	15° 18.735	2204	82	5,2	4,5
30	CTD	16.04.18	13:20	39° 10.993	15° 16.948	2228			
31	Bathy	16.04.18							
32	GC5	17.04.18	06:00	39° 07.443	15° 14.957	2275	73	5	3,08
33	GC5	17.04.18	08:10	39° 07.605	15° 10.628	2442	78	5	2,18
34	GC8	17.04.18	11:00	39° 11.352	15° 11.550	2310	63	2	1,65
35	GC8	17.04.18	12:45	39° 11.510	15° 11.504	2310	67	2	1,84
36	CTD	17.04.18	14:30	39° 11.296	15° 14.468	2285			
37	Bathy	17.04.18							
38	GC8	18.04.18	06:01	39° 11.436	15° 14.496	2285	83	8,3	6,74
39	GC8	18.04.18	08:20	39° 11.328	15° 08.696	2303	80	8	6,17
40	GC8	18.04.18	11:00	39° 12.333	15° 04.309		70	6	5,82
41	CTD	18.04.18	13:30	39° 13.505	15° 13.059	2346			
42	Bathy	18.04.18							
43	GC8	19.04.18	07:20	39° 11.954	14° 56.519	3150	71	3,5	2,45
44	GC8	19.04.18	11:00	39° 09.946	14° 57.543	3145	82	3	2,35
45	Bathy	19.04.18							
46	GC8	20.04.18	06:00	39° 08.427	15° 13.434	2294	78	8	5,45
47	GC8	20.04.18	08:26	39° 09.071	15° 07.715	2482	88	8,3	7,44
48	GC8	20.04.18	11:02	39° 10.744	15° 02.547	2103	72	7	6,84
49	Bathy	20.04.18							
50	CTD	21.04.18	06:00	38° 57.556	15° 22.493				
51	GC8	21.04.18	08:00	39° 01.180	15° 24.075	2112	72	5	1,74
52	GC8	21.04.18	11:07	39° 05.348	15° 06.051	2606	62	0	0
53	GC8	21.04.18	13:16	39° 06.123	15° 05.692	2583	68	0	0
54	Bathy	21.04.18							
55	GC3	22.04.18	06:05	39° 04.838	15° 00.677	2891	67	0	0
56	GC3	22.04.18	09:10	39° 15.797	14° 53.760	3183	82	3	1,84
57	Dredge	23.04.18	06:00	38° 52.216	14° 55.979	2300			
58	Dredge	23.04.18	11:03	38° 51.302	15° 03.056	2054			
59	Dredge	24.04.18	06:00	38° 50.292	14° 55.880	1977			
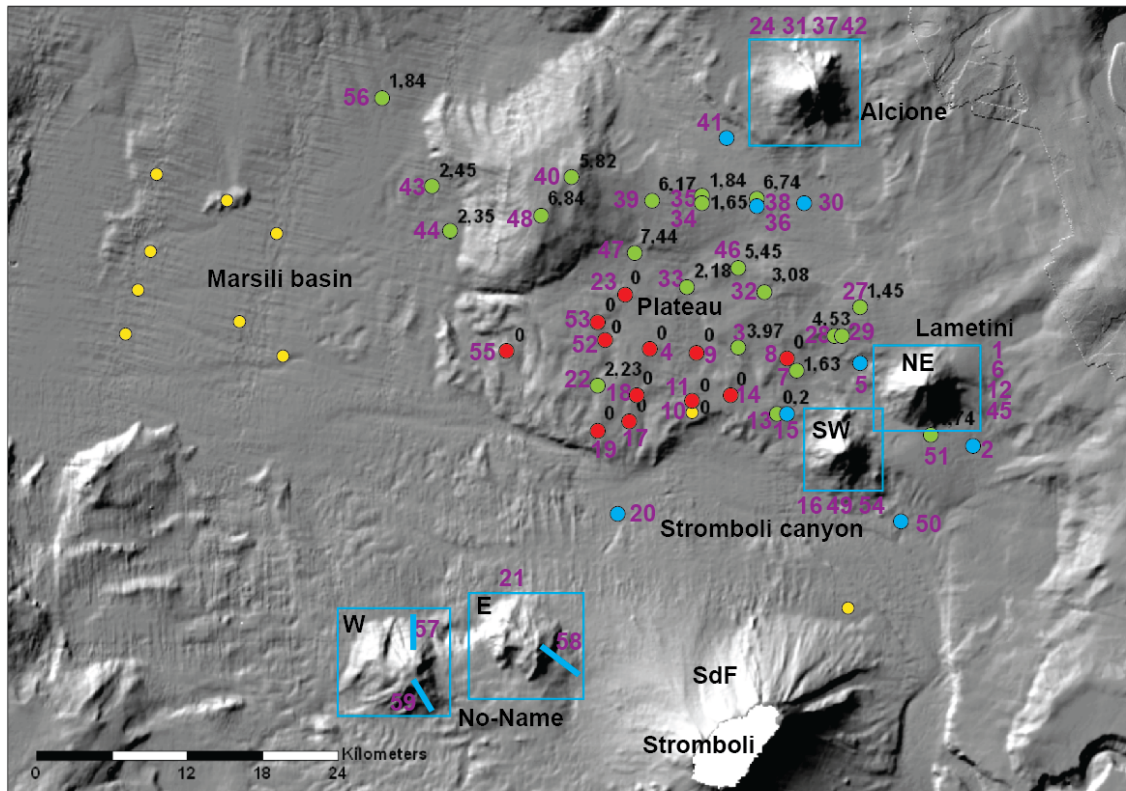
Fig. 3: Map of stations. Violet station numbers refer to 4.2. Blue boxes are bathymetric mapping areas each comprising several stations. Blue bars are dredge tracks. Blue dots are CTD deployments. Green dots are gravity coring sites with recovery shown in [m]. Red dots are sites with no recovery. Yellow dots are successful cores from earlier expeditions available for the project at ISMAR Bologna.

5. Seamounts: bathymetry and dredge sampling

Little is known about the five seamounts (arranged in three groups) north and west of Stromboli. A volcanic origin of the Alcione and Lemetini seamounts had be demonstrated by earlier dredging whereas no samples had yet been recovered from the No-Name seamounts. Bathymetric mapping aimed to investigate the structure of these semaounts.

During RV Poseidon cruise POS522 multibeam mapping was carried out by a Seabeam 3000 series echosounder system (SB3100) provided by ELAC Nautik GmbH. The SeaBeam 3100 multibeam echosounder (MBES) collects bathymetric, corrected backscatter, side scan and water column imaging (WCI) data at medium depths. It has an across-ship swath width of up to 140 degrees with up to 630 beams for each multi-ping. The complete system consists of 2 transmitter/ receiver units, a motion sensor (Coda Octopus F180), and a salinometer installed on RV Poseidon. The system was operated with HydroStar v4.0. Data acquisition was performed with Hypack 2016. The Hysweep survey module of Hypack bundle collected all data from the SeaBeam echo sounder in HSX data format which was used for further processing. Since the HSX data contain all necessary information for post processing work the native ELAC XSE-data format was not stored during the cruise.

The configuration installed on RV Poseidon operates in the 50 kHz frequency band at water depths ranging from 3 m below the transducers to approximately 3,000 m. However, beside this theoretical value we observed that the best operation depth under optimal weather conditions is between >100 m to <2000 m water depth. The Alcione and Lemetini seamounts lie at 800 to 2200 m water depths. Repeated mappings and careful adjustment of the data acquisition by several CTD salinity and sound-velocity profiles measured near the mapping

areas allowed us to obtain bathymetric maps of sufficient resolution to observe their tectonic structure. However, mapping at the No-Name seamounts at 2500-2900 m water depths did not produce satisfying results.
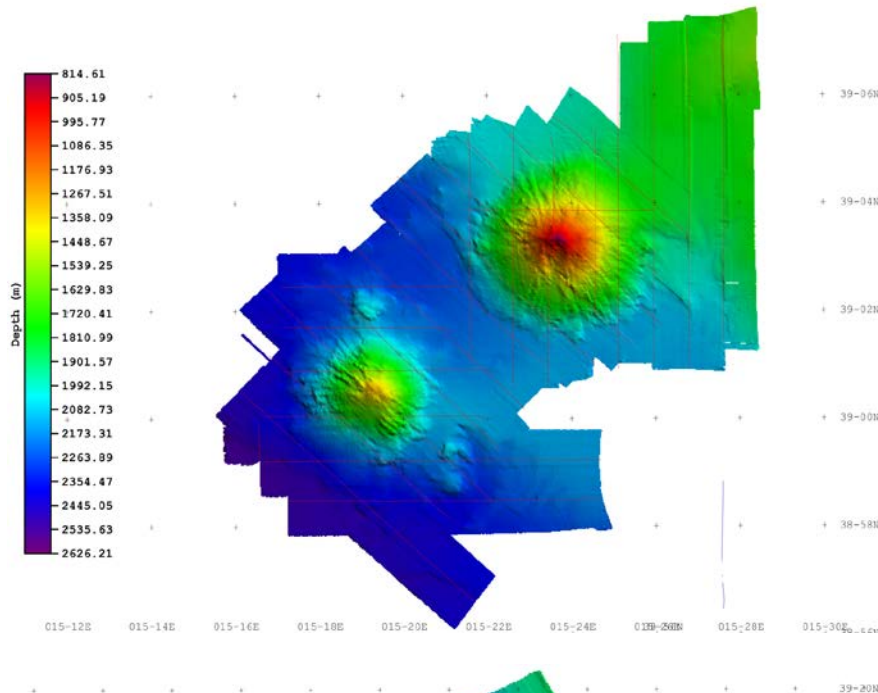

Fig. 4: Bathymetrc map of the Lametini seamounts. Red lines mark the mapping tracks.

Both Lametini seamounts have circular cone shapes with central summits. The Lametini NE seamount reveals a narrow collapse scarp extending from the summit southward down to the foot of the volcano.
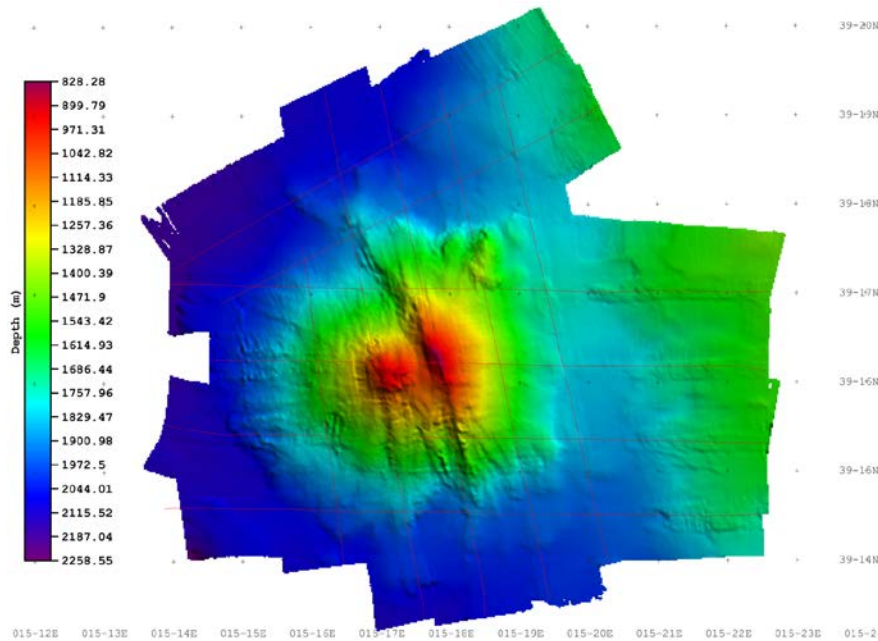

Fig. 5: Bathymetrc map of the Alcione seamount. Red lines mark the mapping tracks.

The Alcione seamount lies on the continental slope leading down into Marsili basin. It is about 1 km high and dissected by a large NNW-SSE striking regional normal fault with a vertical throw of 900 m. Water column imaging (WCI) of the multibeam system identified rising gas bubble swarms above the fault as well as above the summit of the western cone indicating continued magmatic/tectonic activity at Alcione.
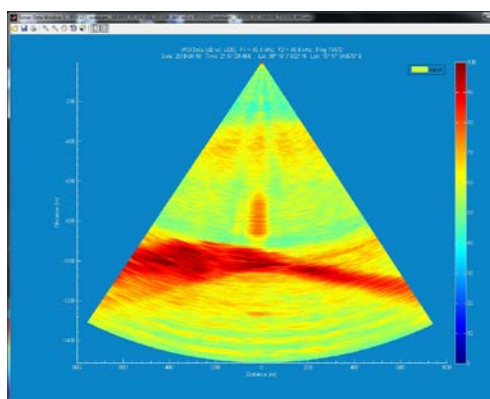

Fig. 6: WCI image of a gas bubble swarm (orange region at center above red ground) above the Alcione fault.

The three dredges collected at the No-Name seamounts were heavily loaded with mud including brown/black fragmented incrustation levels. Only the dredge at station 58 at the SE flank of No-Name E seamount recovered hard rock fragments. These include px-fsp-phyric pillow lava fragments with vesicular interior and dense crust, rounded moderately vesicular gray lapilli rich in amphibole and clear feldspar phenocrysts as well as an amphibole megacryst fragment (3 cm), glassy fluidally textured lava chips, a few well-rounded pumice lapilli, and fragments of weakly solidified well-sorted sandy hyaloclastite. Therefore the No-Name seamounts are most likely also of volcanic origin and relatively young considering the fresh state of the rock samples, despite the apparently thick cover of mud that reflects the very high sediment accumulation rates at the south rim of the Stromboli canyon.
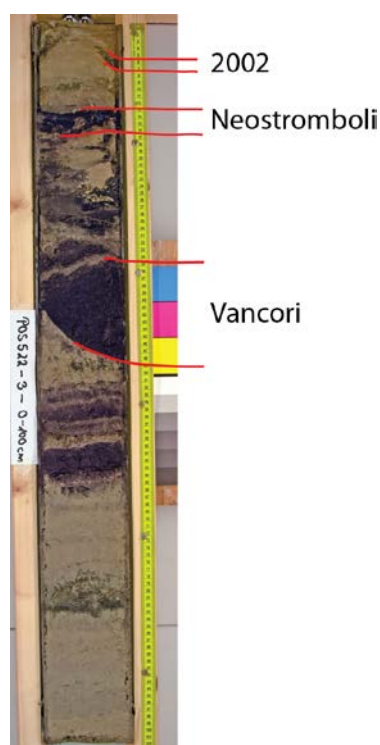
6. Gravity Coring Results

Fig. 7: Top 1 m segment of core station 3 showing major black turbidite layers with erosional unconformities.

Fig. 8: W-E profile of core across the northern plateau. Red lines connect Vancori (V) and Neostromboli (NS) turbidites, violet lines connect underlying white ash, blue lines tentatively connect older volcaniclastic turbidites. See Fig. 3 for station positions.

All cores that recovered at least the upper 1 m of sediment contain two major black sandy turbidite layers (Fig. 7) which have been tentatively correlated to the major known collapse events at Stromboli, the 13 ka Vancori and the 5 ka Neostromboli collapses (Fig. 2). In addition, thin turbidite layers on top of these have been observed in many cores and represent younger, weaker events such as the one in 2002. However, all correlations still need to be verified by geochemical comparisons.
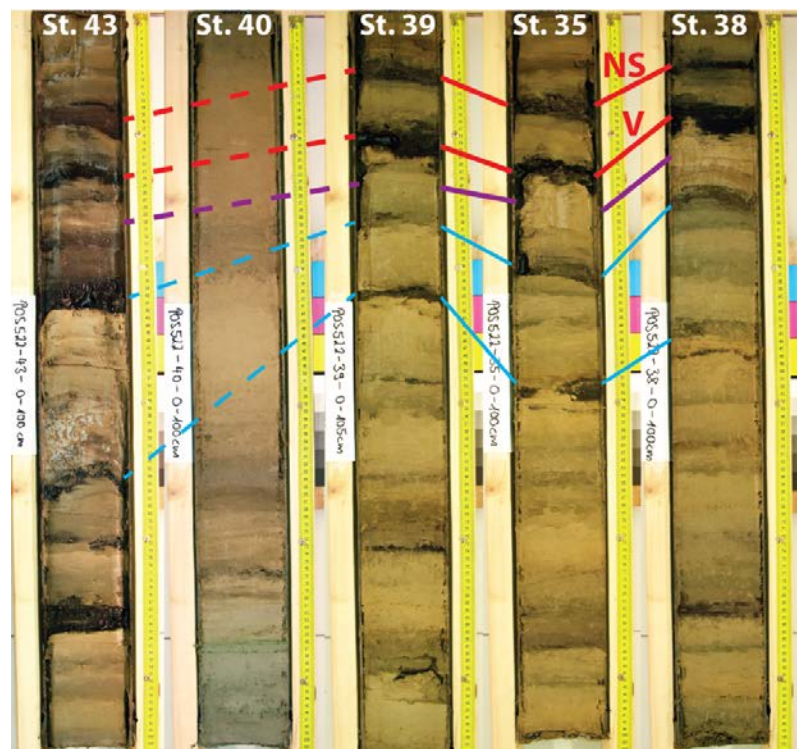
An exception are stations 51, 56 and 40. Station 51 south of Lametini NE seamount only contains continent-derived turbidites which are characterized by containing abundant mica, and this station marks the eastern dispersal limit of the Stromboli turbidity currents. Similarly, station 56 in the northeast corner of the Marsili basin marks the northern limit of volcaniclastic turbidite dispersal as it also only contains

mica-rich continental turbidites. Station 40 lies on top of a submarine hill at the northwest edge of the plateau (Fig. 3) and was apparently too high above the surrounding seafloor for significant turbidity current deposition (Fig. 8).
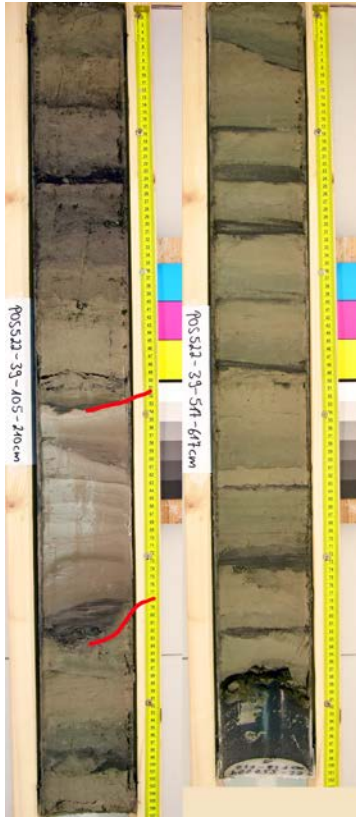

Fig. 9: Two segments of core 39. Left: red lines bracket presumed Campanian Ignimbrite turbidite 158-188 cm bsf. Right: Bottom section of the core with greenish pelagic sediments intercalated with black volcaniclastic turbidite layers.

Across the southern, proximal half of the plateau particularly the Vancori and Neostromboli turbidites are apparently too thick and too close to the seafloor for penetration by the gravity corer which typically flipped over when hitting the ground. Hence almost all coring attempt yielded no recovery except black sand and mud in the core catcher. Across the northern half of the plateau, however, the turbidite layers can be traced along the cores. For example, Figure 8 show a W-E transect along stations 43, 40, 39, 35 and 38 (Fig. 3). The Vancori and Neostromboli layers have very similar thickness and appearance along this profile indicating that the turbidity currents spread evenly across the plateau and into Marsili basin but were unable to surmount the hilltop at station 40.

The cores contain several volcaniclastic turbidite layers intercalated in the sediments below the 13 ka Vancori turbidite (Fig. 8). It appears that these can also be correlated between the cores and have similar wide spread suggesting that these may also have been significant collapse events.

The cores also contain abundant primary ash beds. For example, a white ash beds underlies the Vancori turbidite (Fig. 8) and is tentatively correlated with a major eruption on Lipari. Another prominent example is the thick white pumiceous turbidite package at 160 cm bsf in core 39 (Fig. 9), which could be the submarine equivalent of the 39 ka Campanian Ignimbrite. Once such correlation can be geochemically verified, they will provide important time markers in the core stratigraphies.

Long cores (e.g., station 39, Fig. 9) have recovered sediment packages including green reduced intervals that seem to reach back through glacial times. These are intercalated with black volcaniclastic turbidite layers at intervals on the order of 10 cm. Analysis of these cores will eventually help to better understand the evolution of Stromboli through the late Pleistocene which appears to have involved numerous collapse events. In addition, paleo-environmental analyses of the sediments should provide data to test for any systematic relationship between turbidite frequency (and possibly magnitude) and environmental changes.

7. Final notes

Both work and archive halves of all cores have been stored in the cooled GEOMAR core repository and will be available for further sampling and studies. These studies will also make use of sediment cores from the same region obtained by earlier cruises and stored at ISMAR Bologna. The new bathymetric data is available through both the GEOMAR and ISMAR Bologna data storages.

8. References

Carey S, Maria T, Cornell W (1998) Processes of volcaniclastic sedimentation during the early growth stages of Gran Canaria based on sediments from Site 953. In: Weaver PPE, Schmincke HU, Firth JV, Duffield W (eds), Proc ODP Sci Res 157: 183-200

Di Roberto A, Rosi M, Bertagnini A, Marani MP, Gamberi F (2010) Distal Turbidites and Tsunamigenic Landslides of Stromboli Volcano (Aeolian Islands, Italy). In: Mosher DC et al. (eds) Submarine mass movements and their consequences. Advances in natural and technological Hazards Resaerch 28, Springer Media BV: 719-731

Garcia MO (1996) Turbidites from slope failures on Hawaiian volcanoes. In: MCGuire WJ, Jones AP, Neuberg J (eds.), Volcano instability of the Earth and Other Planets. Spec Pub Geol Soc London 110: 281–292

Garcia MO, Meyerhoff Hull D (1994) Turbidites from giant Hawaiian landslides: Results from Ocean Drilling Program Site 842. Geology 22: 159-162

Hampton MA (1972) The role of subaqueous debris flow in generating turbidity currents. J sedim Pet 42: 775-793

Hunt JE, Talling PJ, Clare MA, Jarvis I, Wynn RB (2014) Long-term (17 Ma) turbidite record of the timing and frequency of large flank collapses of the Canary Islands. Geochem Geophys Geosyst 15 (8): 3322-3345

Hunt JE, Wynn RB, Croudace IW (2015) Identification, correlation and origin of multistage landslide events in volcaniclastic turbidites in the Moroccan Turbidite System. In: Micro-XRF Studies of Sediment Cores - Applications of a non-destructive tool for the environmental sciences, Developments in Paleoenvironmental Research 17: 147-172, DOI:10.1007/978-94-017-9849-5_5

Kokelaar P, Romagnoli C (1995) Sector collapse, sedimentation and clast population evolution at an active island-arc volcano: Stromboli, Italy. Bull Volc 57: 240–262

Maramai A, Graziani L, Alessio G, Burrato P, Colini L, Cucci L, Nappi R, Nardi A, Vilardo G (2005a) Near- and far-field survey report of the 30 December 2002 Stromboli (Southern Italy) tsunami. Mar Geol 215: 93–106

Maramai A, Graziani L, Tinti S (2005b) Tsunamis in the Aeolian Islands (southern Italy): a review. Mar geol 215: 11-21

Marani MP, Gamberi F, Rosi M, Bertagnini A, Di Roberto A (2008a) Deep-Sea Deposits of the Stromboli 30 December 2002 Landslide. In: The Stromboli Volcano: An Integrated Study of the 2002-2003 Eruption. Geophysical Monograph Series 182: 157-169

Marani MP, Gamberi F, Rosi M, Bertagnini A, Di Roberto A (2008b) Subaqueous density flow processes and deposits of an island volcano landslide (Stromboli Island, Italy). Sedimentology, doi: 10.1111/j.1365-3091.2008.01043.x

Murty TS (2004) Tsunami wave height dependence on landslide volume. Pure Appl Geophys 160: 2147–2153

Piper DJW, Cochonat P, Morrison ML (1999) The sequence of events around the epicentre of the 1929 Grand Bank earthquake: initiation of debris flows and turbidity current inferred from sidescan sonar. Sedimentology 46:79-97

Tibaldi A (2001) Multiple sector collapses at Stromboli volcano, Italy: how they work. Bull Volcanol 63: 112–125

Tinti S, Bortolucci E, Armigliato A (1999) Numerical simulation of the landslide-induced tsunami of 1988 on Vulcano Island, Italy. Bull Volcanol 61: 121-137

Tinti S, Bortolucci E, Romagnoli C (2000) Computer simulations of tsunamis due to sector collapse at Stromboli, Italy. J Volcanol Geotherm Res 96: 103-128

Tinti S, Manucci A, Pagnoni G, Armigliato A, Zaniboni F (2005) The 30 December 2002 landslide-induced tsunamis in Stromboli: sequence of the events reconstructed from the eyewitness accounts. Nat Haz Earth Sys Sci 5: 763–775